ChemComm

Accepted Manuscript

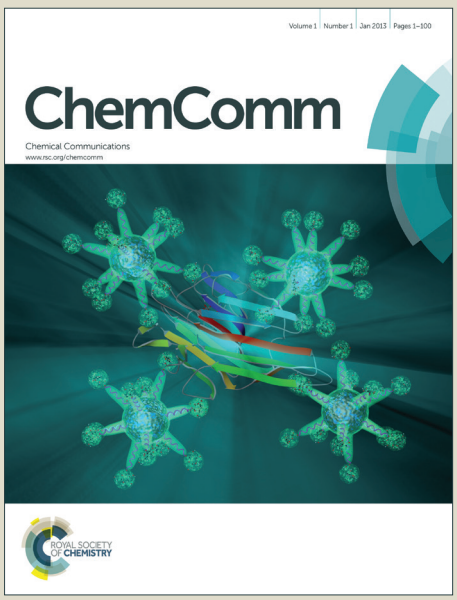

ROYAL SOCIETY OF CHEMISTRY

www.rsc.org/chemcomm

ChemComm

RSCPublishing

COMMUNICATION

Photochemical synthesis of size-tailored hexagonal ZnS quantum dots†

Cite this: DOI: 10.1039/x0xx00000x

Carlos M. Gonzalez,[a] Wei-Chen Wu,[b] Joseph Tracy, [b] Benjamin Martin [a]*

Received 00th January 2012,
Accepted 00th January 2012

DOI: 10.1039/x0xx00000x

www.rsc.org/

ZnS quantum dots were synthetized at room temperature using a simple photochemical process involving ketyl radicals. Through the simple adjustment of reagent concentration, the method allows the control of nanoparticle size. Transmission electron microscopy confirmed that the nanomaterial adopts the hexagonal structure.

The search for synthetic routes to nanoparticulate ZnS has received substantial attention over the last three decades owing to its important technological applications, which include its use in photodetectors, light emitting diodes, phosphors, fluorescent markers for biological applications, photocatalysts, *etc*.[1-5] In particular, the pursuit of facile chemical routes to ZnS quantum dots (QDs) has drawn a great deal of effort given the dependence of the electronic properties with size when the dimension of the material is comparable to the Borh radius.[6-7] For ZnS, the bulk band gap is 3.66 eV, which corresponds to an absorption maximum located approximately at 340 nm.[8] For ZnS, the Borh radius is estimated to be 5.5 nm,[9-10] which implies that important quantum confinement effects should be reflected in the optical properties of ZnS nanoparticles (NPs) with sizes below this threshold. In this size range, the absorption maximum progressively shifts to the blue with further reduction of size.[11] This allows the design of emitting and absorbing materials with specific ranges of absorption and emission wavelengths by controlling the size, morphology, and crystal structure of the nanomaterial.

Solvothermal methods have been widely used for the production of ZnS NPs.[2,12-14] Ultrasonication,[15] reverse micelles,[16] and radiolysis methods[9] have also been successfully employed. The study of photochemical routes to chalcogenides has also been addressed.[17-25] Ketyl radicals generated photochemically using aromatic ketones have been employed for the etching of surface material in CdSe and CdSe/ZnS NPs.[26-27] However, in spite of important practical advantages, the photochemical routes have not been extensively exploited for the production of ZnS QDs. It is important to stress that photochemistry also allows the production of nanoparticulate material at room temperature. The power of the photochemical route employed in this work has been recently demonstrated through the production of bimetallic and anisotropic Au-containing nanoparticles.[28]

In this study, we report the photochemical synthesis of ZnS QDs using the reducing power of 2-hydroxyl-isopropyl radicals ($[E(CH_3COCH_3,H^+/(CH_3)_2\dot{C}-OH) = -1.4$ V *vs.* NHE]),[29] resulting from the photochemically initiated hydrogen transfer reaction between acetone and isopropanol, **Scheme 1**. The mechanism of photoreduction of ketones to the formation of ketyl radicals has been thoroughly investigated.[30-34]

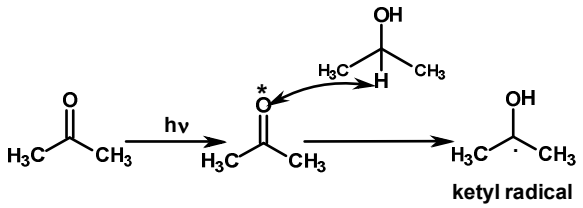

Scheme 1. Photochemical formation of ketyl radicals

ZnS QDs were prepared by UV irradiation (260-400 nm range, with maximum at 280 nm, and fluency in the 200 fc range) of an isopropanol solution containing $Zn(CH_3COO)_2$ and thiourea in presence of acetone. Nanoparticles of varying radii were synthetized from solutions containing $[Zn(CH_3COO)_2]$ = 1, 10 and 25 mM. For all the experiments the molar ratio thiourea : $Zn(CH_3COO)_2$ = 10, and [acetone] = 1 M. The photolysis time was 30 minutes for every case. The process resulted in the formation of a white product, which is characteristic of ZnS. At low concentration of $Zn(CH_3COO)_2$ (1mM), the product remained suspended resulting in a cloudy and homogenous dispersion that was stable for 8 – 10 hours. Increasing amounts of $Zn(CH_3COO)_2$ (10 and 25 mM) resulted in the formation of a milky system that aggregated progressively. For all of the preparations, the formation of ZnS readily occurred within 10

[a] *NSF-PREM Center for Interfaces in Materials*
Department of Chemistry and Biochemistry,
Texas State University
601 University Drive
San Marcos, TX 78666
[b] *North Carolina State University*
Department of Materials Science and Engineering
911 Partners Way
Raleigh, NC 27695

†Electronic Supplementary Information (ESI) available: See DOI: 10.1039/c000000x/

minutes of irradiation, and the reaction was completed in 20-30 minutes. The concentration of acetone used (1 M) aimed at the promotion of short photolysis times while preserving the target NP dimensions. At the irradiation intensity employed, lower amounts of acetone did not affect the size. The use of acetone at stoichiometric concentrations (with respect to both $Zn(CH_3COO)_2$ and thiourea) produced ZnS, but the process took 1 - 2 hours to be completed. It is worth mentioning that prolonged irradiation of solutions containing both $Zn(CH_3COO)_2$ and thiourea in absence of acetone did not result in a chemical reaction. In fact, it was found that solutions of thiourea in isopropanol are highly photostable but progressively decompose upon UV irradiation when acetone has been added to the system, pointing to the intermediacy of ketyl radicals in the process.

In this synthesis, thiourea was used as the sulfur source, as the stabilizing ligand, and as a size modifier. The ratio $Zn(CH_3COO)_2$: thiourea was optimized to produce ZnS QDs populations with narrow size distribution. For all the target sizes, a ratio equal to 10 resulted suitable to produce samples with small size dispersion. For this ratio, the reaction yield was determined using conventional gravimetry. The reaction yield for the photolysis of a 30 mL sample containing 10 mM $Zn(CH_3COO)_2$, 100 mM thiourea and 1 M acetone was 81 % (the yield was calculated by product mass after centrifugation and rinsing with isopropanol). Therefore, the optimization of the molar ratio of reagents aiming at the production of ZnS samples with low size dispersion also promoted the formation of a large amount of material. For every studied system, a ratio below 5 did not result in the formation of ZnS in the allowed photolysis time. For the case of the system with $Zn(CH_3COO)_2$ concentration equal to 1 mM, intermediate ratios of thiourea (5 – 9 mM range) produced noticeable amounts of ZnS nanomaterial with optical properties outside the expected range. The use of greater ratios of thiourea : $Zn(CH_3COO)_2$ (>10) did not seem to offer any improvement for nanoparticle size or stability.

For the as-prepared material, transmission electron microscopy confirmed the formation of ZnS QDs (size < 5 nm), Figure 1 a-c. The TEM micrographs reveal a dependence of nanoparticle size with $[Zn(CH_3COO)_2]$. For the system where $[Zn(CH_3COO)_2]$ = 1mM, the nanoparticle size is 1.9±0.6 nm; for $[Zn(CH_3COO)_2]$ = 10 mM, 2.8±0.7 nm; and for 25 mM, 4.1±1 nm. Histograms representing the size distribution for the sample populations in Figure 1 a-c may be found in Figure S1 (ESI). Electron diffraction measurements (Figure 1d) revealed that the as-prepared material is hexagonal ZnS. The lattice spacing as estimated from the high-resolution image (Figure 1e), d = 0.23 nm, correspond to the lattice plane (102). Figure 1e also shows the interception angle (~ 63 °) between planes in the hexagonal array (expected value = 60 °). Fast Fourier transform (Figure 1f) from the image in Figure 1e clearly shows a 6-fold symmetry. X-ray energy dispersive spectroscopy measurements of the ZnS material upon centrifugation and rinsing resulted in an atomic ratio Zn-to-S ≈ 1. X-ray diffraction measurement (ESI, Figure S2) of an annealed sample (200 °C) prepared with 10 mM $Zn(CH_3COO)_2$ and 100 mM thiourea also indicates the formation of ZnS. The estimated crystallite size using the Scherrer equation was 2.5 nm, which is in agreement with the nanoparticle size regime in TEM imaging (Figure 1b). As has been reported elsewhere, it was not possible to identify the lattice for the as-prepared ZnS based on XRD measurements given the similar 2θ values for the corresponding reflections of both the hexagonal and cubic systems, as well as the poorly resolved XRD profile characteristic of nanomaterials.[2,35]

The formation of a hexagonal lattice for the photochemically prepared ZnS QDs was not expected since the favored phase below 1023 °C is the cubic phase.[13,36] In our reaction conditions, the formation of ZnS QDs consistently occurred as early as 10 minutes, clearly indicating that the photochemical process takes place at a significantly higher reaction rate than its thermal counterparts.[2,14] The relative monodispersity of the particles indicates that the nucleation stage occurs rapidly and homogeneously, and that the seeds also grow rapidly to consume the reagent. It is not clear why this process results in hexagonal ZnS, but previous reports indicated that it is possible to synthesize hexagonal ZnS at lower temperature.[2,14,37-44] Note that for all the cited reports the reaction T was > 150°C.

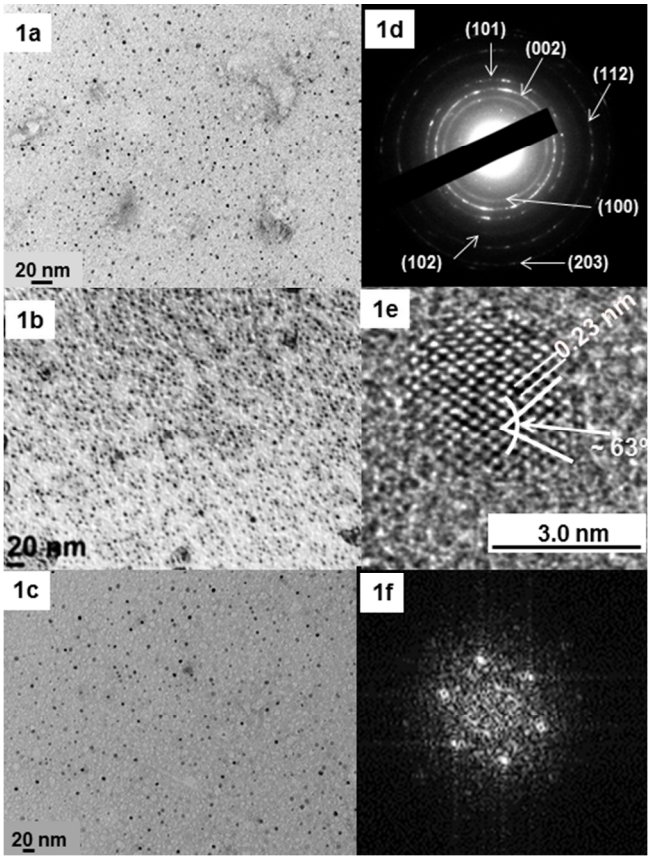

Figure 1. TEM images for the as-prepared ZnS QDs. 1a) Sample prepared with 1 mM $Zn(CH_3COO)_2$ (mean size 1.9±0.6 nm); 1b) sample prepared with 10 mM $Zn(CH_3COO)_2$ (2.8± 0.7 nm); 1c) sample prepared with 25 mM $Zn(CH_3COO)_2$ (4.1±1.0 nm); 1d) electron diffraction pattern for a representative sample; 1e) high resolution image for a sample prepared using 1 mM $Zn(CH_3COO)_2$; and 1f) the corresponding FFT image.

Figure 2a shows UV spectra of representative ZnS samples upon separation of material from the reaction media and redispersion in isopropanol (the absorbance, A_c, was corrected for Tyndall scattering). The absorption profiles show a dependence upon the used $[Zn(CH_3COO)_2]$ and reveals the action of quantum confinement effects. Note that the absorption bands possibly contain a component from strongly bound thiourea ligands. Thermogravimetric analysis of a ZnS QDs sample (Figure S3, ESI) reveals a significant weight loss (~ 26 %) starting at 150 °C, at the decomposition temperature range of thiourea.[45] This suggests that thiourea plays a chief role in the stabilization of the nanomaterial. The excitation spectra (Figure 2b) were obtained by monitoring the emission at 400 nm. The position of the excitation maxima agrees with previous size correlations of optical properties for ZnS QDs.[11,46-48] The excitation bands are narrow, which suggests a low size dispersion. These observations indicate that, in spite of the absence of added stabilizing and size

control reagents other than an excess of thiourea, the method offers size control. For all of the cases under study, the emission was recorded upon excitation at 300 nm. For each target concentration of $Zn(CH_3COO)_2$, the emission maximum is located at 400 nm. Interestingly, the emission profile of the as-prepared ZnS QDS does not change either with $[Zn^{2+}]$ or with increasing concentration of thiourea (that is, with a molar ratio thiourea : Zn^{2+} > 10). For every sample, a large stoke shift for the emission band is present (arising from the recombination of charge carriers from a trap-state). This indicates the operation of non-radiative de-excitation pathways before the emission of electromagnetic radiation takes place (trap-state emission). It should be noted that the absence of a direct excitonic emission is common for ZnS nanomaterials.[10,47,49-50] The trap-state emission with maximum at 400 nm has been related to the intermediacy of surface Zn^{2+} vacancies. A slight shoulder at 430 nm can also be observed. The latter emission component has been linked to the trapping action of sulfur vacancies.[50-51] For all of the as-prepared material, the excitation spectrum monitoring at 430 nm resulted in the excitation band as for the excitation scan monitoring at 400 nm. This indicates that this emission component originates from the same excitonic state as the emission at 400 nm, ruling out the existence of a population of NPs with a different size range.

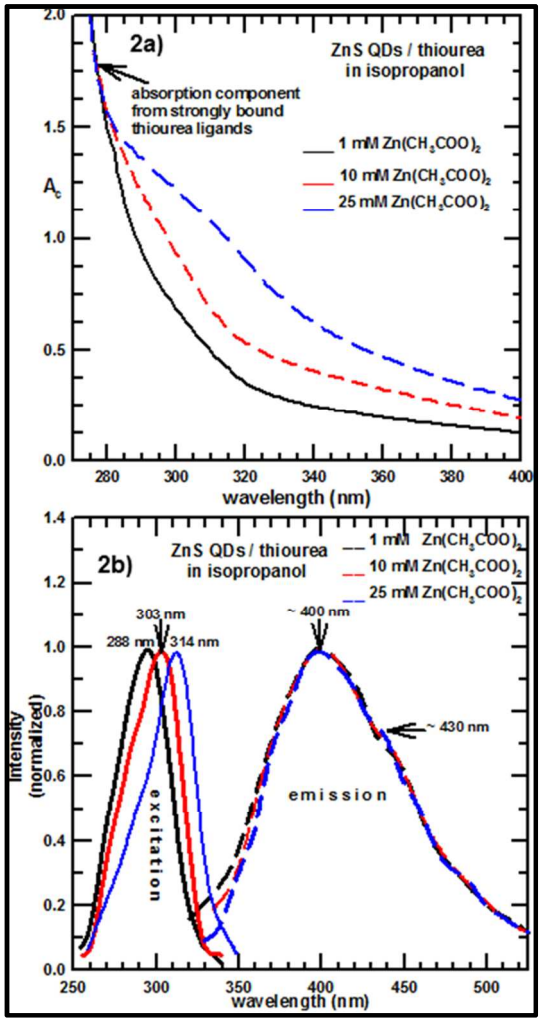

Figure 2. a) UV spectra for the ZnS QDs (diluted to 0.4 mM in isopropanol) prepared with $[Zn(CH_3COO)_2]$ = 1, 10, 25 mM using a thiourea-to-$Zn(CH_3COO)_2$ ratio = 10. b) Excitation scans and emission spectra for the ZnS QDs samples, (for emission measurements, the samples were diluted in isopropanol to 0.1 mM).

A detailed reaction mechanism for the process employed here has not yet been established. However, some mechanistic information can be discussed through the analysis of the results and the available literature. Ketyl radicals are capable of reducing Zn^{2+} [E^o (Zn^{2+}/Zn^o) = - 0.76 V]. However, Zn^0 would be rapidly oxidized in a protic solvent such as isopropanol. As discussed previously, thiourea is highly photostable but will photodegrade in presence of acetone. Ten hours of irradiation with UV light of a solution of thiourea in either isopropanol or acetone did not promote any noticeable chemical change (as evidenced by the unchanged UV spectrum with irradiation time); in contrast, in the presence of both acetone and isopropanol, the concentration decreased progressively with irradiation until disappearance (Figure S4, ESI). This points to the chief action of reducing ketyl radicals in the photodecomposition of thiourea, and the resulting formation of sulfur atoms. This is consistent with previous observations that reduction of thiourea analogs using pulsed radiolysis result in the formation of thiol species (R-SH) and thiol derivatives upon the formation of thiolate radicals (R-S•).[52-53] Likewise, the reduction of thiourea by hydrogen atoms (H•) generated by sonochemical means was found to promote the formation of H_2S.[54]

A proposed reaction sequence responsible for the formation of ZnS is shown in Scheme 2. It is possible that in the experimental conditions used for this study, ketyl radicals promoted the formation of S^{2-} species through a series of electron transfer reactions analogous to those described above.[9,52] The electron transfer process in Equation 1 should convert thiourea to a thiolate radical containing a carbanion center, which should be rapidly quenched by the acidic media created because of the oxidation of the isopropanol radical ($(CH_3)_2\dot{C}{-}OH \rightarrow CH_3COCH_3 + H^+ + e^-$). The net result should be a thiol radical, R-S•, and acetone (as represented in Equation 1). This should be followed by a hydrogen transfer reaction (Equation 2), generating a ketyl radical from isopropanol and a thiol species (R-SH).[30] The resulting unstable thiol should decompose, (Equation 3) to produce sulfide species (H_2S, HS^-, S^{2-}). Finally, H_2S will react with Zn^{2+} to generate ZnS QDs (Equation 4). We note that it is possible that some of the byproduct sulfide species (*e.g.* thiols, sulfide species) contributed to the stabilization of the nanoparticulate ZnS system, which would help to explain the high size control and high nanoparticle stability that this process achieved in spite of the absence of added stabilizers.

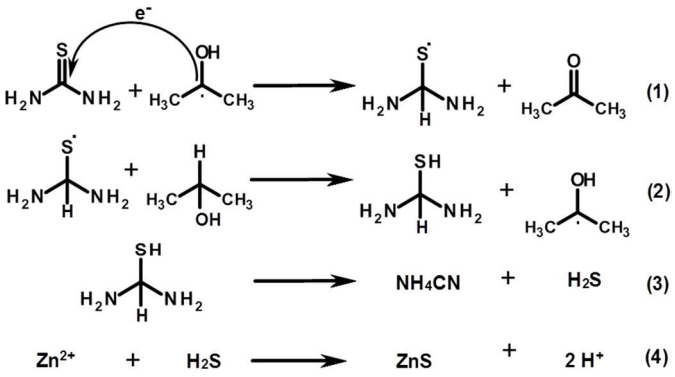

Scheme 2. Proposed reaction sequence involved in the formation of ZnS QDs.

To the extent of our knowledge, this is the first report accounting for both the formation of hexagonal ZnS QDs at room temperature, and the use of ketyl radicals for the production of semiconducting nanoparticles. In addition, the method allows the size control of the ZnS quantum dots with excellent reproducibility, and a high reaction yield. The merits

of this methodology include the simplicity (*i.e.* one-step process, room temperature, size control by the simple adjustment of reagent concentrations, and reproducibility), and the low cost of the process (in terms of reducing agents and energy consumption). The process has the additional advantages of the reforming of acetone. It is also important to mention that the irradiation level employed in the outlined experiment was not particularly intense, as it is comparable to the radiance originating in a regular 100-110 V fluorescent lamp (300 fc). This work hints, too, at the potential of the photochemical methods in the production of materials that at present can only be prepared at high temperature, e.g. transition metal chalcogenides and intermetallic compounds of transition metals.

We thank the National Science Foundation (PREM Center for Interfaces, DMR-1205670, and Research Triangle MRSEC, DMR-1121107) for the financial support of this research. We acknowledge the support of the National Science Foundation for X-ray (CRIF: MU-0946998), SEM and TEM (National Science Foundation, DUE-9052039) instrumentation, and the patronage of the Wells Foundation (AI-0045). The authors also acknowledge the use of the Analytical Instrumentation Facility at North Carolina State University.

Notes and references

1. Monroy, E.; Omnès, F.; Calle, F. Semicond. *Sci. Technol.* **2003**, 18, *R33-R51*.
2. Zhao, Y.; Zhang, Y.; Zhu, H.; Hadjipanayis, G. C.; Xiao, J. Q. *J. Am. Chem. Soc.* **2004**, *26*, *6874-6875*.
3. Chen, R.; Lockwood, D. J. J. *Electrochem. Soc*. **2002**, 149, *S69-S78*.
4. Hui Li, Wan Y. Shih, and Wei-Heng Shih. *Ind. Eng. Chem. Res.* **2010,** 49, *578-582*.
5. Bredol, M.; Kaczmarek, M. *J. Phys. Chem. A* **2010**, 114, *3950-3955*.
6. Alivisatos, A. P. *J. Phys. Chem*. **1996**, 100, *13226-13239*.
7. Burda, C.; Chen, X.; Narayanan, R.; El-Sayed, M.A. *Chem. Rev.* **2005**, 105, *1025-1102*.
8. Fan, F.-R. F.; Leempoel, P.; Bard, A. J. *J. Electrochem. Soc*. **1983**, 130, *1866-1875*.
9. Souici, A.H.; Keghouche, N.; Delaire, J.A.; Remita, H.; Mostafavi, M. *Chem. Phys. Lett.* **2006**, 422, *25-29*.
10. Jovanović, D.J.;.Validžić, I. L.; Janković, I. A.; Bibić, N.; Nedeljković. J. M. *Mater.Lett.* **2007**, 61, *4396–4399*.
11. Nakaoka, Y.; Nosaka, Y. *Langmuir* **1997**, 13, *708-713*.
12. Wilhelmy, D. M.; Matijević, E. *J. Chem. Soc., Faraday Trans. 1*, **1984**, 80, *563-570*.
13. Williams, R.; Yocom, P. N.; Sofko, F. S. *J. Colloid Interface Sci.* **1985**, *106*, *388-398*.
14. Yu, S-H.; Yoshimur, M. *Adv. Mate*r. **2002**, 14, *296-299*.
15. Geng, J.; Liu, B.; Xu, L.; Hu, F. N.; Zhu, J. J. *Langmuir* **2007**, 23, *10286–10293*.
16. Zhang, J.; Xiao, M.; Liu, Z.; Han, B.; Jiang, T.; He, J.; Yang G. *J. Colloid Interface Sci.* **2004**, 273, *160-164*.
17. Stroyuk, A. L.; Shvalagin, V. V.; Raevskaya, A. E. ; Kryukov, A. I.; Kuchmii. S. Y. *Theor. Exp. Chem.* **2008**, 44, *205-231*.
18. Cheon, J.; Zink, J. I. *J. Am. Chem. Soc*. **1997**, 119, *3838–3839*.
19. Ichimura, M.; Goto, F.; Arai, E. *J. Appl. Phys*. **1999**, 85, 7411.
20. Wang, C. Y.; Mo, X.; Zhou, Y.; Zhu, Y. R.; Liu, H. T.; Chen. Z. Y. *J. Mater. Chem.* **2000**, 10, *607–608*.
21. Wu, S.-D.; Zhu, Z.; Zhang, Z.; Zhang, L. *Mater. Sci. Eng. B* **2002**, 90, *206-208*.
22. Marandi, M.; Taghavinia, N.; Iraji, A. ; Mahdavi, S. M. *Nanotechnology* 2005**, 16,** *334-338*.
23. Ren, T.; Xu, S.; Zhao, W.-B.; Zhu, J.-J. *J. Photochem. Photobiol. A* **2005**, 173, *93-98*.
24. Ichimura, M.; Goto, F.; Ono, Y.; Arai, E.; *J. Crystal Growth* **1999**, 198-199, *308-312*.
25. Wang, C. Y.; Mo, X.; Zhou, Y.; Zhu, Y. R.; Liu, H. T.; Chen, Z. Y. *J. Mater. Chem*. **2000**, 10, *607-608*.
26. Galian, R. E.; de la Guardia, M.; Perez-Prieto, J. *J. Am. Chem. Soc*. **2009**, 131, *892-893*.
27. Galian, R. E.; de la Guardia, M.; Perez-Prieto, J. *Langmuir* **2011**, 27, *1942-1945*.
28. Gonzalez, C. M.; Martin, B.; Betancourt, Tania. *J. Mater. Chem. A.*, **2014**, 2, *17574-17585*.
29. Batchelor, S. N. *New. J. Chem.* **2004**, *28*, *1200*.
30. Turro, N. J. *Modern Molecular Photochemistry*. University Science Books: Sausalito, California, **1991**.
31. Grotewold, J.; Soria, D.; Previtali, C.M.; Scaiano, J.C. *J. Photochem*. **1972–1973**, 1, *471*.
32. Laroff, G. P.; Fisher, H. *Helv. Chem. Acta.* **1973**, 45, *506*.
33. Zeldes, H.; Livingston, R. *J. Chem. Phys*. **1966**, 45, *1946*.
34. Nakashima, M.; Hayon. E. *J. Phys Chem*. **1971**, *75*, *1910*.
35. Biswas, S.; Kar, S. *Nanotechnology* **2008**, 19**,** *045710*.
36. Qadri, S. B.; Skelton, E. F.; Hsu, D.; Dinsmore, A. D.; Yang, J.; Gray, H. F.; Ratna, B. R. *Phys. Rev. B* **1999**, 60, *9191-9193*.
37. La Porta, F. A.; Andrés, J.; Li, M. S.; Sambrano, J. R.; Varela J. A.; Long, E. *Phys. Chem. Chem. Phys*. **2014**, 16, *20127-20137*.
38. Huang, F.; Banfield, J. F. *J. Am. Chem. Soc*. **2005**,127*, 4523-4529*.
39. Sun, J.-Q.; Shen, X.-P.; Chen, K.-M.; Liu, Q.; Liu, W. *Sol. State Communications* **2008**, 147, *501-504*.
40. Tong, H.; Zhu, Y.-J.; Yang, L.-X.; Li, L.; Zhang, L.; Chang, J.; An, L.-Q.; Wang, S.-W. *J. Phys. Chem. C* **2007**, 111, *3893-3900*.
41. Acharya, S. A.; Maheshwari, N.; Tatikondewar, L.; Kshirsagar, A.; Kulkarni, S. K. *Cryst. Growth Des*. **2013**, 13, *1369-1376*.
42. Deng, Z.-X.; Wang, C.; Sun, X.-M.; Li, Y.-D. *Inorg. Chem.* **2002**, 41, *869-873*.
43. Vogel, W. *Langmuir* **2000**, 16, *2032−2037*.
44. Zhang, H.; Gilbert, B.; Huang F.; Banfiel, J.F. *Nature*, **2003**, 424, *1025−1029*.
45. Wang, S.; Gao, Q.; Wang, J. *J. Phys. Chem. B* **2005**, *109, 17281-17289*.
46. Nanda, J.; Sapra, S.; Sarma, D. D. *Chem. Mater*. **2000**, 12, *1018−1024*.
47. Souici, A. H.; Keghouche, N.; Delaire, J.A.; Remita, H.; Mostafavi, M. *Chem. Phys. Lett.* **2006**, 422, *25–29*.
48. Kumbhojkar, N.; Nikesh, V. V.; Kshirsagar, A.; Mahamuni, S. *J. Appl. Phys*. **2000**, 88, *6260-6264*.
49. Wang, Y.; Zhang, L.; Liang, C.; Wang, G.; Peng, X. *Chem. Phys. Lett.* **2002**, 357, *314-318*.
50. Lu, H-Y.; Chu, S-Y.; Tan S.-S. *J. Cryst. Growth* **2004**, 269, *385-391*.
51. Wageh, S.; Ling, Z. S.; Xu-Rong, X. *J. Cryst. Growth* **2003**, 255, *332-337*.
52. Dey, G.R.; Dwibedy, P.; Naik, D.B.; Kishore, Kamal; Moorthy, P.N. *Res. Chem. Intermed*. **1999,** 25, *403-410*.
53. Swayambunathan, V.; Hayes, D.; Schmidt, K. H.; Liao, Y. X.; Meisel, D. *J. Am. Chem. Soc*. **1990**, 112, *3831-3837*.
54. Wang, C-L.; Zhang, H.; Zhang, J. H.; Li, M. J.; Sun H. Z., Yang, B. *J. Phys. Chem. C* **2007**, 111*, 2465-2469*.

